Adaptive transcriptional strategies underpin the host-specific virulence of the generalist oomycete *Phytophthora capsici* during early crown infection

Pablo Vargas-Mejía[1,2,3], Lino Sánchez Segura[4], Fernando U. Rojas-Rojas[1,2], Harumi Shimada-Beltrán[1,2] and Julio C. Vega-Arreguín[1,2*]

[1]Laboratorio de Ciencias AgroGenómicas, Escuela Nacional de Estudios Superiores Unidad León, UNAM, Blvd. UNAM 2011, 37684, León, México.

[2]Laboratorio Nacional PlanTECC, Escuela Nacional de Estudios Superiores Unidad León, UNAM, Blvd. UNAM 2011, 37684, León, México.

[3]Posgrado en Ciencias Biológicas, Universidad Nacional Autónoma de México, CDMX, México.

[4]Centro de Investigación y de Estudios Avanzados del Instituto Politécnico Nacional. Unidad Irapuato, km. 9.6, Libramiento Norte, Carretera Irapuato-León, Guanajuato, 36824, México.

***Corresponding author:** JCVA (jvega@enes.unam.mx)

Abstract

Phytophthora capsici is a destructive, broad-host-range oomycete responsible for substantial losses in global agriculture. While most transcriptomic studies have focused on host responses, the mechanisms by which generalist pathogens dynamically adapt their infection programs to diverse plant species remain poorly understood. Here, we present a comparative transcriptomic analysis of *P. capsici* during early-stage crown infection in four taxonomically and immunologically distinct hosts, *Cucumis sativus, Cucumis melo, Capsicum annuum* (CM334), and *Solanum lycopersicum*, via RNA-seq and multiphoton microscopy. Focusing on crown infections, the natural entry point for the pathogen, we reveal host-specific transcriptional programs that underpin differential infection strategies and outcomes.

Our data show that *P. capsici* exhibits tightly regulated, host-dependent deployment of key virulence factors, including RxLR, NLP, and CRN, and elicitin effectors and reprograms its metabolism to exploit host-specific nutritional environments. In rapidly necrotizing hosts such as tomato, the pathogen induces glycolytic and fatty acid pathways while repressing immunogenic effectors. In contrast, cucurbits support prolonged biotrophic colonization, accompanied by the

upregulation of carbohydrate metabolism and membrane transport genes. In the partially resistant chili pepper CM334, *P. capsici* shows signs of metabolic stress, cell wall remodeling, and effector repression, which is consistent with failed invasion.

Functional validation via RNAi-mediated silencing of selected effectors revealed distinct roles in modulating virulence and host necrosis, confirming the functional relevance of the transcriptomic profiles. Co-expression network analysis uncovered discrete transcriptional modules associated with tissue-specific colonization, nutrient acquisition, and immune evasion.

These results reveal how a generalist soil-borne pathogen finely tunes its gene expression in response to host-specific constraints, revealing conserved and host-specific transcriptional strategies that drive infection success or failure. This work provides mechanistic insight into adaptive virulence and expands our understanding of host-pathogen compatibility in eukaryotic microbes.

Keywords: *Phytophthora capsici*; Host-pathogen interactions; Effector regulation; Metabolic reprogramming; Oomycete pathogenesis; Virulence strategies; Generalist pathogen

1 Background

Phytophthora capsici is a notorious filamentous phytopathogenic oomycete responsible for severe symptoms in vegetable, ornamental, and tropical crops, such as root and stem rot, reduced size in plants, and necrosis (Quesada-Ocampo et al. 2023). These symptoms lead to a yield decrease and, in severe cases, the loss of crops around the world. (Lamour et al. 2012b). As a soil-borne pathogen with a broad host range, *P. capsici* infects several species of the *Cucurbitaceae* and *Solanaceae* families, causing the first symptoms of diseases in the root, such as root rot and subsequent stem blight and fruit rot. *P. capsici* displays adaptative strategies to colonize its hosts, and it is considered a generalist phytopathogen; it has a highly adaptable infection strategy, allowing it to overcome diverse plant defense mechanisms (Quesada-Ocampo et al. 2023). Despite its importance, our understanding of the molecular mechanisms underlying host-specific infection strategies remains incomplete. Most of the previous studies have focused on plant transcriptomic responses to *P. capsici*, and fewer have investigated how the pathogen modulates its gene

expression in response to different hosts and infection niches, providing valuable insights into pathogen adaptation and virulence (Chen et al. 2013; Jupe et al. 2013; Maillot et al. 2022). In addition, most transcriptomic studies of *P. capsici* have focused on foliar infection, even though this pathogen naturally enters plants mostly through soil and colonizes roots and the crown region (Hausbeck and Lamour 2004). The crown infection niche presents unique physiological and immunological features in terms of its structural characteristics, nutrient availability, and composition of host defense mechanisms that may influence pathogen gene expression and virulence strategies (Knight and Sutherland 2016; Stephens et al. 2008).

The early infection stage is particularly critical, as *P. capsici* must rapidly establish and grow within host tissues while evading recognition by host immune receptors. Pathogen success during this phase depends on the precise regulation of effector proteins, metabolic reprogramming, and stress adaptation mechanisms (Judelson 2017; Wang et al. 2023; Zuluaga et al. 2016). Notably, effector proteins such as RxLRs and Crinklers (CRNs) play essential roles in suppressing plant immune responses, whereas secreted hydrolytic enzymes facilitate tissue colonization (Chepsergon et al.; Stam et al. 2021; Wang et al. 2023; Zuluaga et al. 2016). On the other hand, metabolic plasticity also plays a key role, as *P. capsici* must exploit host-derived nutrients while resisting the oxidative stress imposed by plant defenses (Judelson 2017).

Despite these advances, the host-dependent transcriptomic responses of *P. capsici* remain poorly characterized, particularly in the context of crown infections in multiple hosts. Comparative transcriptomics of the pathogen across different plant species can reveal core virulence determinants as well as host-specific adaptations that shape infection outcomes. Understanding how *P. capsici* fine-tunes its gene expression in response to diverse host environments is crucial for developing targeted disease management strategies.

The aim of this study was to elucidate the transcriptomic responses of *P. capsici* during infection of four host species: two cucurbitaceous hosts (cucumber and melon) and two solanaceous hosts (CM334 chili pepper and tomato). Notably, our experimental design focused on infections initiated at the crown of the plant rather than the more commonly examined foliar infections. This approach is particularly relevant given that *P. capsici* is a soil-borne pathogen that exploits the crown region

to establish systemic colonization. By investigating the transcriptomic profiles of *P. capsici* in these hosts at the early infection stage, we aimed to provide insights into the molecular determinants of host-specific virulence, as well as the metabolic adaptations that facilitate successful colonization.

2 Results

2.1 Host susceptibility and stem colonization

To evaluate host susceptibility to *P. capsici* D3, we infected the crowns of *C. annuum* (Criollo de Morelos 334 chili pepper), *C. melo* (melon), *C. sativus* (cucumber), and *S. lycopersicum* (tomato) plantlets with mycelia. The representative phenotypes of 5–8-week-old plants at 24 hours post-inoculation (hpi) are shown in Figure 1a-d. Among the tested hosts, cucumber exhibited the most pronounced aerial mycelial growth (Figure 1a-d), followed by melon and subsequently chili pepper and tomato. Interestingly, the extent of mycelial growth on the surface of the infected tissue contrasted with the time required for the pathogen to induce necrosis in the cucumber melon and tomato plants (Figure 1e).

The tomato was the most susceptible host; the first symptoms of necrosis were observed at 12 hpi for some individuals, and the median time for infected plants to show necrosis was 27 hpi, reflecting rapid progression of the infection. In contrast, the cucurbitaceous hosts displayed symptoms of necrosis at later times post-inoculation. Melon plants started to show necrosis at 36 hpi, with the median time of symptom appearance in the melon plant population at 54 hpi, whereas cucumber plants began to necrose at 48 hpi, reaching median necrosis onset at 102 hpi. Notably, chili pepper (CM334), a genotype previously reported to be partially resistant to *P. capsici* infection, exhibited an even further delayed necrotic response, with the first symptoms evident at 90 hpi and a median necrosis onset at 120 hpi (Figure 1e).

Despite delayed necrosis induction, in cucurbitaceous plants, greater intercellular mycelial growth was observed in these hosts during the sampling period. At 24 hpi, stem cross-sections dissected from 1 cm above the inoculation area showed abundant intercellular *P. capsici* D3 mycelial growth, particularly in vascular tissues, in an apoplastic manner (Figure 1f, g; Figure S1). In the tissue, the solophenyl (channel green) and propidium iodide (channel red) stains the cell walls of the plants and mycelia of *P. capsici* D3, respectively.

The tomato plants exhibited large mycelial growth. Unlike cucurbitaceous plants, the pathogen grows longitudinally into the surrounding parenchyma tissue but does not invade the vascular tissue (Figure 1i). Interestingly, the chili pepper plants did not exhibit intercellular mycelial growth in their stem tissues at 24 hpi (Figure 1h). Further examination of the inoculation site and 1 cm distal stems at 48 hpi confirmed that *P. capsici* D3 could not penetrate or invade chili pepper tissues effectively at these time points prior to necrosis (Figure S2).

2.2 Tissue-Specific Infection Dynamics: Root and Stem

To evaluate the tissue-specific pattern of infection, we examined intercellular mycelial growth in the roots of infected melon and chili pepper seedlings. At 24 hpi, *P. capsici* exhibited low proliferation in the roots of melon, and at 48 hpi, the pathogen showed a small increase in root colonization (Figure 2a). This could suggest that the pathogen had greater affinity for stems than for roots (Figure 1f-i and 2c-d).

Consistent with observations at the stem, mycelial growth was not detected in chili pepper roots even when the pathogen developed appressoria at 24 and 48 hpi (Figure 2b and S3). At 96 hpi, infection progression resulted in *P. capsici* mycelial growth extending into the aerial photosynthetic parts of tomato; at 120 hpi in melon and cucumber; and at 144hpi in pepper chili plantlets. This observation suggests that *P. capsici* tends to colonize the aerial portions of its hosts, despite initial zoospore deposition being concentrated at the crown, roots, and stem base under field conditions (Figure S4).

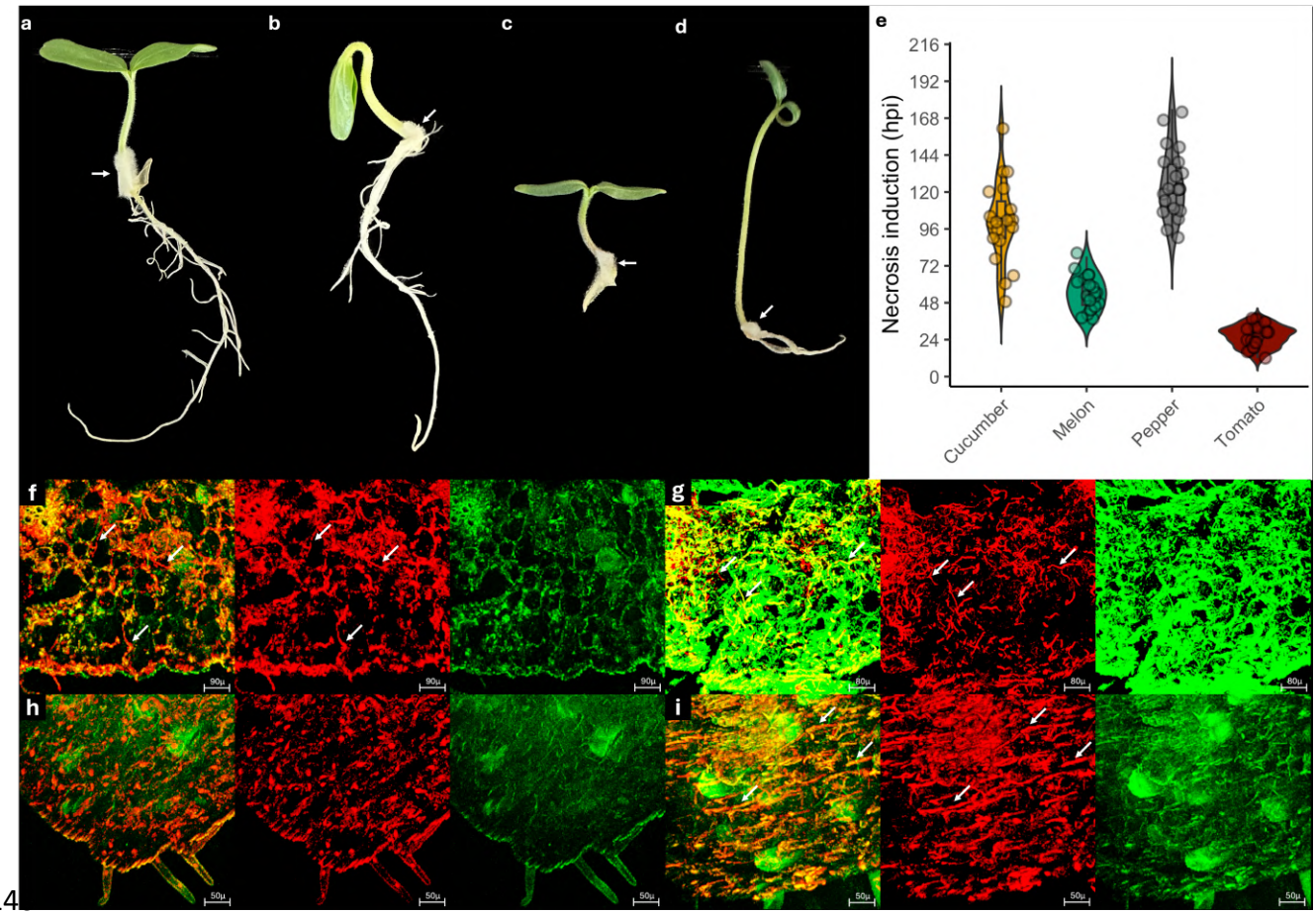

Figure 1: Dynamics of *P. capsici* infection. **a** Cucumber (24 hpi). **b** Melon (24 hpi). **c** Chili pepper (24 hpi). **d** Tomato (24 hpi). **e** Time to necrosis induction by the host. **f** 3D reconstruction of a stem section of a cucumber infected plant at 24 hpi. **g** 3D reconstruction of a stem section of a melon infected with *P. capsici* at 24 hpi. **h** 3D reconstruction of infected Chili pepper stem section (24 hpi). **i** 3D reconstruction of a stem section of a tomato infected with *P. capsici* (24 hpi). White arrows highlight portions of mycelium. The plant cell wall was stained with solophenyl flavine (green channel), and the hyphae of *P. capsici* were stained with propidium iodide (red channel). For each host, the left image presents both channels, the middle image presents only propidium iodine staining, and the right panel presents only the solophenyl channel.

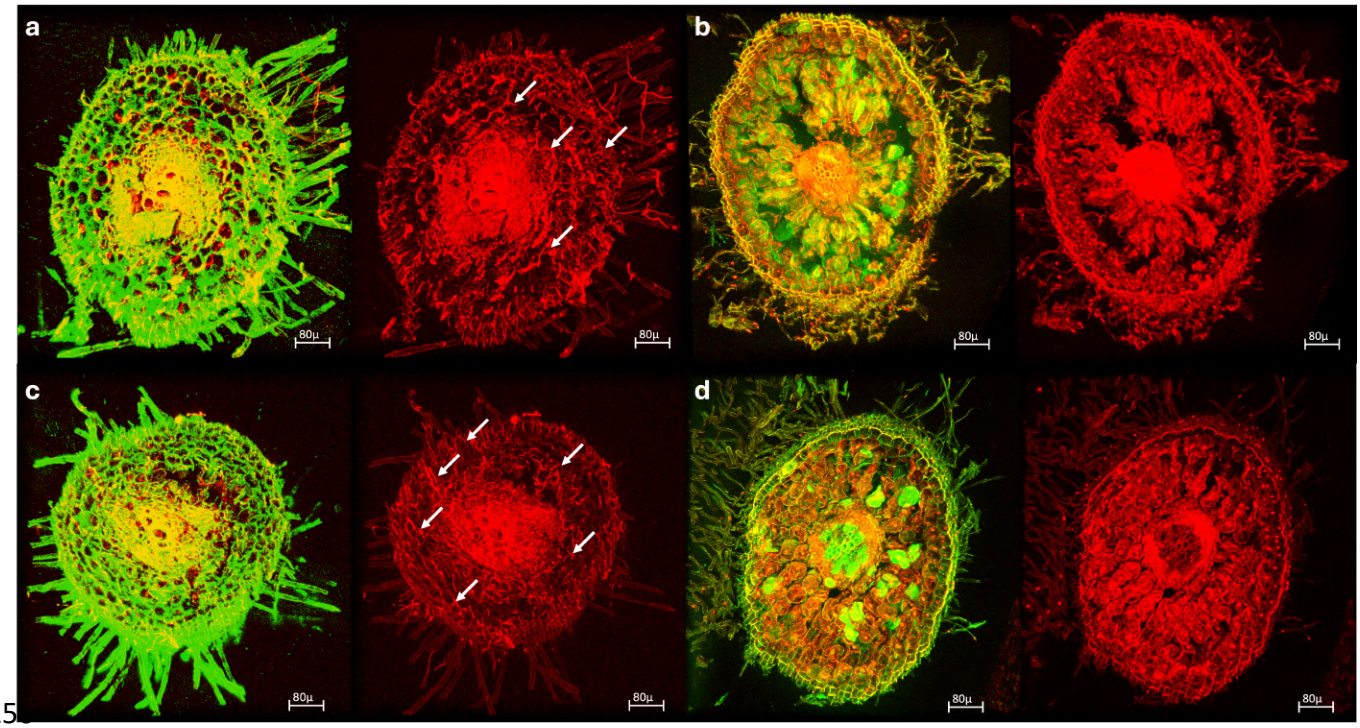

Figure 2: Root colonization of *P. capsici*. **a** 3D reconstruction of melon root at 24 hpi. **b** 3D reconstruction of chili pepper root at 24 hpi. **c** 3D reconstruction of melon root at 48 hpi. **d** 3D reconstruction of chili pepper root at 48 hpi. White arrows highlight portions of mycelium. The plant cell wall was stained with solophenyl flavine (green channel), and the hyphae of *P. capsici* were stained with propidium iodide (red channel). For each host, the left image presents both channels, and the right image presents only propidium iodine (PI) staining.

2.3 Comparative transcriptomic analysis reveals host-dependent pathogenic strategies

We decided to perform RNA-Seq of *P. capsici* infecting Solanaceous and Cucurbitaceous hosts to understand the transcriptional response of the pathogen to the diverse environments that each host represents. Mapping to the reference transcriptome yielded an average mapping rate of 77% for each library. After principal component analysis, we found an evident separation of the transcriptome responses of the *Phytophthora* samples when the pathogen was infecting a host compared with the pathogen growing in V8 agar media (Figure 3a). Additionally, PCA showed an aggrupation of the transcriptomic responses of the cucurbits and tomato infections, although 1 tomato sample was grouped with the chili pepper samples (Figure 3a).

Table 1: Differentially expressed genes*

Condition	Total genes	Up regulated	Down regulated
Cucumber	2270	1281	989
Melon	2366	1167	1199
Chili pepper	2872	1268	1604
Tomato	2104	1104	1000
Total Unique	4470	2226	2307

*padj < 0.05 Log2FC > 1 OR < -1

Among the 19805 transcripts of *P. capsici*, 4470 genes were found to be differentially expressed (DEGs = padj < 0.05 and Log2FC > 1 OR < -1) among all the conditions compared with our control pathogen growing in V8 media (Table 1). We found, on average, approximately 2300 DEGs for each sample, with tomato infections resulting in fewer differentially expressed genes and chili pepper infections resulting in the most differentially expressed genes (Table 1). Among the 4470 DEGs, only 436 were induced among all the conditions, and 415 were down-regulated, indicating that the core transcriptome of *P. capsici* infecting four different hosts is not composed of a large number of genes (Figure 3b, c). This core set of DEGs shared across all *P. capsici* infection conditions was subjected to Gene Ontology (GO) and Kyoto Encyclopedia of Genes and Genomes (KEGG) pathway enrichment analyses to identify key biological processes and pathways involved in plant-pathogen interactions. Among the biological processes, significant enrichment was observed for processes associated with metabolic activity, including fatty acid metabolism, carbohydrate metabolic processes, and glycolysis, alongside defense-related processes such as pathogenesis and electron transport (Figure S5a). Additionally, terms related to cell wall modification and phosphate transport were prominent, reflecting infection and nutrient acquisition by the pathogen.

Pathway enrichment analysis revealed a diverse range of metabolic pathways (Figure S5b). These included fatty acid beta-oxidation, glycolysis/gluconeogenesis, and amino acid metabolism, suggesting a reconfiguration of primary metabolic networks during infection. Notably, pathways associated with the mobilization of nutrients from the host, such as glycerolipid and galactose metabolism, were upregulated, emphasizing the pathogen's strategy to exploit host resources. In

198 parallel, the enrichment of pathways related to defense mechanisms, including alkaloid
199 biosynthesis and gamma-hexachlorocyclohexane degradation, underscores the activation of plant
200 immune responses. The differential enrichment of these pathways among the upregulated and
201 downregulated DEGs provides insights into the dynamic interplay between metabolic
202 reprogramming and adaptation to host defense during *P. capsici* infection.
203
204 The transcriptional response of *P. capsici* revealed remarkable adaptability to the unique micro
205 ecological niches generated by its hosts. While some processes are shared, the pathogen's specific
206 enrichment varies considerably, reflecting its ability to exploit host-specific vulnerabilities and
207 overcome distinct physiological and defense barriers.
208
209 In solanaceous hosts, particularly tomato, *P. capsici* prioritized pathways associated with rapid
210 energy acquisition, such as glycolysis and fatty acid metabolism. This metabolic change was
211 probably due to the faster strategy of pathogen colonization, which corresponds to the host's early
212 necrotic response. Interestingly, during tomato infection, *P. capsici* is also enriched in alkaloid
213 degradation pathways, suggesting that the pathogen may counteract host-produced antimicrobial
214 compounds, including alkaloids, to establish infection. The capacity of *P. capsici* to degrade these
215 compounds highlights the intense chemical warfare between tomato and *P. capsici*, with the
216 pathogen leveraging its metabolic flexibility to neutralize host defenses (Figure 3d, e).
217
218 In contrast, infection of the partially resistant chili pepper CM334 resulted in a distinct pattern of
219 transcriptional enrichment in the pathogen (Figure 3). Processes related to cell wall modification
220 and lipid metabolism were notably upregulated in *P. capsici* during its attempted colonization of
221 chili pepper. These enrichments, including pathways such as terpenoid and glycerolipid
222 metabolism, suggest that *P. capsici* was preparing to breach structural barriers and colonize the
223 host. However, the absence of detectable pathogen growth within chili pepper tissues at 24 hpi
224 (Figure 1c and h) implies that the mechanism of infection was insufficient to overcome the physical
225 and biochemical defenses of this plant. Additionally, the enrichment of nitrogen compound
226 metabolism pathways in *P. capsici* during chili pepper infection may indicate an effort to adapt to
227 nutrient scarcity, reflecting a limitation imposed by host resistance mechanisms.
228

229 Melon infection was characterized by strong enrichment in carbohydrate metabolism, including
230 the galactose and glycerolipid pathways, and processes such as nitrogen utilization and protein
231 glycosylation (Figure 3d, e). These adaptations demonstrate the capacity of the pathogen to use
232 the host's abundant resources to support its growth and effector production. Similarly, in cucumber,
233 *P. capsici* was significantly enriched in glycolysis and gluconeogenesis, suggesting an intensified
234 focus on extracting energy and carbon from the host. Pathways related to transport, such as
235 phosphate and copper transport, were also highly enriched in cucurbitaceous hosts. In chili pepper,
236 the pathogen appears to invest heavily in preparatory mechanisms to overcome structural and
237 chemical defenses, albeit unsuccessful in this case. Conversely, in more susceptible hosts, *P.*
238 *capsici* capitalizes on the availability of nutrients and the relative lack of effective defensive
239 barriers to drive its infection forward.
240

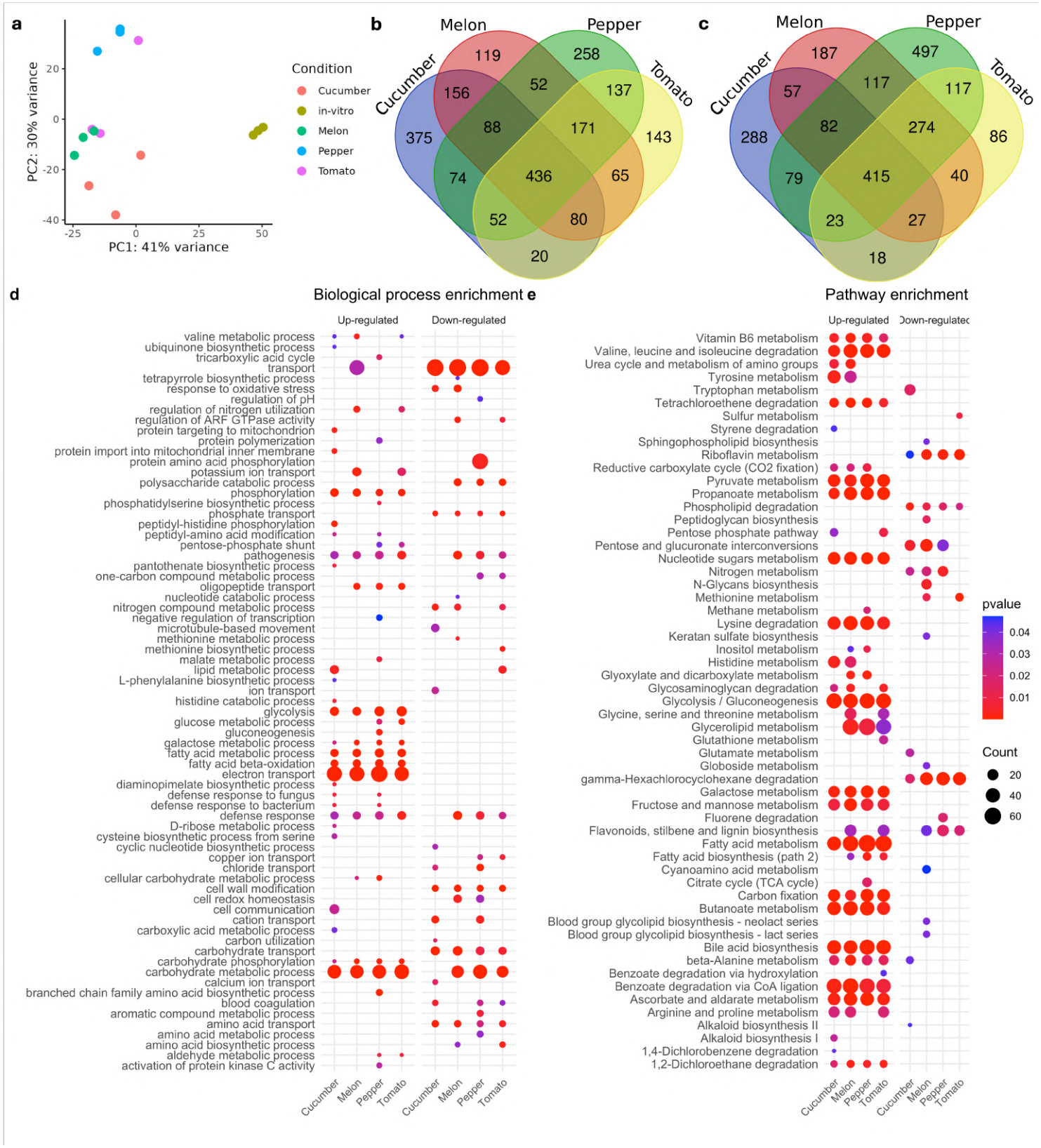
a
PC2: 30% variance
PC1: 41% variance
Condition
Cucumber
in-vitro
Melon
Pepper
Tomato
b
Cucumber
Melon
Pepper
Tomato
119
258
156
52
137
375
88
171
143
74
436
65
52
80
20
c
Cucumber
Melon
Pepper
Tomato
187
497
57
117
117
288
82
274
86
79
415
40
23
27
18
d
Biological process enrichment
Up-regulated
Down-regulated
valine metabolic process
ubiquinone biosynthetic process
tricarboxylic acid cycle
transport
tetrapyrrole biosynthetic process
response to oxidative stress
regulation of pH
regulation of nitrogen utilization
regulation of ARF GTPase activity
protein targeting to mitochondrion
protein polymerization
protein import into mitochondrial inner membrane
protein amino acid phosphorylation
potassium ion transport
polysaccharide catabolic process
phosphorylation
phosphatidylserine biosynthetic process
phosphate transport
peptidyl-histidine phosphorylation
peptidyl-amino acid modification
pentose-phosphate shunt
pathogenesis
pantothenate biosynthetic process
one-carbon compound metabolic process
oligopeptide transport
nucleotide catabolic process
nitrogen compound metabolic process
negative regulation of transcription
microtubule-based movement
methionine metabolic process
methionine biosynthetic process
malate metabolic process
lipid metabolic process
L-phenylalanine biosynthetic process
ion transport
histidine catabolic process
glycolysis
glucose metabolic process
gluconeogenesis
galactose metabolic process
fatty acid metabolic process
fatty acid beta-oxidation
electron transport
diaminopimelate biosynthetic process
defense response to fungus
defense response to bacterium
defense response
D-ribose metabolic process
cysteine biosynthetic process from serine
cyclic nucleotide biosynthetic process
copper ion transport
chloride transport
cellular carbohydrate metabolic process
cell wall modification
cell redox homeostasis
cell communication
cation transport
carboxylic acid metabolic process
carbon utilization
carbohydrate transport
carbohydrate phosphorylation
carbohydrate metabolic process
calcium ion transport
branched chain family amino acid biosynthetic process
blood coagulation
aromatic compound metabolic process
amino acid transport
amino acid metabolic process
amino acid biosynthetic process
aldehyde metabolic process
activation of protein kinase C activity
Cucumber
Melon
Pepper
Tomato
e
Pathway enrichment
Up-regulated
Down-regulated
Vitamin B6 metabolism
Valine, leucine and isoleucine degradation
Urea cycle and metabolism of amino groups
Tyrosine metabolism
Tryptophan metabolism
Tetrachloroethene degradation
Sulfur metabolism
Styrene degradation
Sphingophospholipid biosynthesis
Riboflavin metabolism
Reductive carboxylate cycle (CO2 fixation)
Pyruvate metabolism
Propanoate metabolism
Phospholipid degradation
Peptidoglycan biosynthesis
Pentose phosphate pathway
Pentose and glucuronate interconversions
Nucleotide sugars metabolism
Nitrogen metabolism
N-Glycans biosynthesis
Methionine metabolism
Methane metabolism
Lysine degradation
Keratan sulfate biosynthesis
Inositol metabolism
Histidine metabolism
Glyoxylate and dicarboxylate metabolism
Glycosaminoglycan degradation
Glycolysis / Gluconeogenesis
Glycine, serine and threonine metabolism
Glycerolipid metabolism
Glutathione metabolism
Glutamate metabolism
Globoside metabolism
gamma-Hexachlorocyclohexane degradation
Galactose metabolism
Fructose and mannose metabolism
Fluorene degradation
Flavonoids, stilbene and lignin biosynthesis
Fatty acid metabolism
Fatty acid biosynthesis (path 2)
Cyanoamino acid metabolism
Citrate cycle (TCA cycle)
Carbon fixation
Butanoate metabolism
Blood group glycolipid biosynthesis - neolact series
Blood group glycolipid biosynthesis - lact series
Bile acid biosynthesis
beta-Alanine metabolism
Benzoate degradation via hydroxylation
Benzoate degradation via CoA ligation
Ascorbate and aldarate metabolism
Arginine and proline metabolism
Alkaloid biosynthesis II
Alkaloid biosynthesis I
1,4-Dichlorobenzene degradation
1,2-Dichloroethane degradation
Cucumber
Melon
Pepper
Tomato
pvalue
0.04
0.03
0.02
0.01
Count
20
40
60

242 Figure 3: Transcriptional responses of *P. capsici* to different hosts. **a** Principal component analysis of *P.*
243 *capsici* transcript expression. **b** Venn diagram of up-regulated DEGs. **c** Venn diagram of down-regulated
244 DEGs. **d** Biological process and **e** KEGG pathway enrichment of *P. capsici* differentially expressed genes.
245
246 **2.4 Host-dependent effector expression profiles**
247 We found that 70 RxLRs, 28 Elicitins, 18 CRNs, and 17 NLPs effectors were differentially
248 expressed. RxLR expression was mainly down-regulated except for 12 genes, and its expression
249 was grouped according to the family of the infected host; the same behavior was found for the
250 CRN effectors (Figure 4). However, Elicitins clustered with melon, tomato, and chili pepper, with
251 the cucumber condition as the most different. NLPs expression was clustered for tomato,
252 cucumber, and melon, with chili pepper being the most dissimilar condition for the expression of
253 this effector family. NLPs were also repressed, with only 5 NLPs being overexpressed.
254 A review of the annotated RxLR effectors in our dataset revealed a diverse arsenal with distinct
255 expression patterns that align with previously reported functions. For example, several homologs
256 of PsAvh328 (genes Pc123179, Pc128001, and Pc552887) have been shown in earlier studies to
257 interfere with host defense signaling and modulate immune responses (Wang et al. 2011).
258 Interestingly, while some Avh328 homologs remain unexpressed under some conditions, gene
259 Pc123179 is induced in chili pepper, suggesting a specialized role in overcoming host-specific
260 defenses. Similarly, PsAvh16 (Pc14944, Pc14948, and Pc533084) has been implicated in
261 suppressing programmed cell death, thereby assisting the pathogen in establishing a biotrophic
262 interaction (Fedkenheuer 2016). Gene Pc13391, which encodes the uncharacterized Avh166 gene,
263 is consistently downregulated across all hosts, possibly indicating its involvement at earlier/later
264 infection stages or under environmental cues not captured in our current sampling. The marked
265 downregulation of Pc20942 across conditions may reflect tightly regulated deployment. The
266 effector PcAvh103 (gene Pc536383) has been linked to the manipulation of EDS1, thus facilitating
267 virulence; however, our data revealed that this gene was downregulated in all host infections (Li
268 et al. 2020).
269
270 Our expression analysis of elicitin-encoding genes in *P. capsici* revealed notable variability across
271 host conditions. Several elicitins, including the genes Pc16186, Pc21853, and Pc127268, exhibit
272 robust positive expression in all hosts. However, the gene Pc508761 (annotated as INF2B) is

273 strongly repressed in melon and tomato, and the gene Pc508770 (INF1-like) is not induced in
274 cucumber, chili pepper, or tomato but is moderately repressed in melon. INF1 is one of the best-
275 characterized elicitins and is known in *P. infestans* for its sterol-binding activity and ability to elicit
276 a hypersensitive response in a range of plant hosts (Ah-Fong et al. 2021; Du et al. 2017).
277 Additionally, INF2B is related to triggering HR (Huitema et al. 2005). The observed repression of
278 both INF1 and INF2B in melon and INF2B in tomato suggest that *P. capsici* may actively
279 downregulate these elicitors to avoid triggering host defense responses and avoid necrosis during
280 its biotrophic stage.
281
282 Crinkler (CRN) effectors form a large and diverse family in oomycetes that can manipulate host
283 cell death and immune responses. In our dataset, the CRN125 homolog (gene Pc131973) is
284 strongly expressed in cucumber and melon but is downregulated in chili pepper and not in tomato,
285 suggesting a role tailored to the cucurbit host environment, as proposed to interact with cucurbit
286 TCP14-1 or TCP14-2 to enhance virulence (Stam et al. 2021). Multiple entries annotated as
287 CRN15 show variable patterns; for example, the Pc50894 gene is expressed in both cucumber and
288 melon but not in other hosts, whereas the Pc106668 also annotated as CRN15, is upregulated in
289 melon, chili pepper, and tomato. In contrast, CRN10 (gene Pc506739) is expressed solely in
290 cucumber, and CRN10 homologs (genes Pc109378 and Pc80099) are downregulated in chili
291 pepper and tomato, suggesting distinct regulatory controls even among closely related CRNs.
292 Other CRN annotations, such as CRN77 (gene Pc128631) and CRN34 (gene Pc117855), exhibit
293 modest expression in specific hosts (CRN77 in cucumber and melon and CRN34 prominently in
294 melon), whereas members such as CRN5 (gene Pc540976) and CRN21 (gene Pc133238) show
295 little to no differential expression, possibly reflecting functions that are restricted to particular
296 infection stages or conditions. Pc559084 was induced in all hosts, and this gene was shown to be
297 able to suppress HR triggered by INF1 but increase disease susceptibility in *N. benthamiana* plants
298 (Chen et al. 2015). Many CRNs in *P. capsici* remain uncharacterized. The diverse expression
299 profiles observed here underscore the potential for functional specialization within the CRN family
300 and highlight the need for further research to unravel their roles in host-specific pathogenicity.
301
302 Nep1-like proteins (NLPs) are a diverse family of secreted effectors known to induce necrosis in
303 dicotyledonous plants by binding to membrane glycosylinositol phosphorylceramides (GIPCs)

(Lenarčič et al. 2017). In our dataset, the expression profiles of several NLPs revealed distinct, host-dependent regulation. For example, the gene Pc9358, annotated as PcNLP14, is uniquely induced in chili pepper, whereas its expression does not change in cucumber, melon, or tomato. PcNLP14 was previously shown to be one of the most highly expressed NLP effectors in chili pepper and *N. benthamiana,* and its agroinfiltration in plants resulted in the induction of necrosis (Feng et al. 2014). In contrast, the Pc122048 gene was moderately induced in both cucumber and melon but was not differentially expressed in chili pepper and tomato. Pc129784 PcNLP2, another inducer of necrosis, is exclusively induced in cucumber, further supporting host-specific functions among NLPs (Chen et al. 2018). On the other hand, several NLPs, including the gene Pc107869 and its close homolog gene Pc108964, are consistently repressed in melon, chili pepper, and tomato, indicating that their expression could be tightly controlled to avoid premature host cell death (Chen et al. 2018). Other NLPs, such as Pc108039 NLP4 and Pc119748 NLP6, exhibit strong repression specifically in chili pepper and melon, whereas the genes Pc18373 and Pc69122 are downregulated across all hosts.

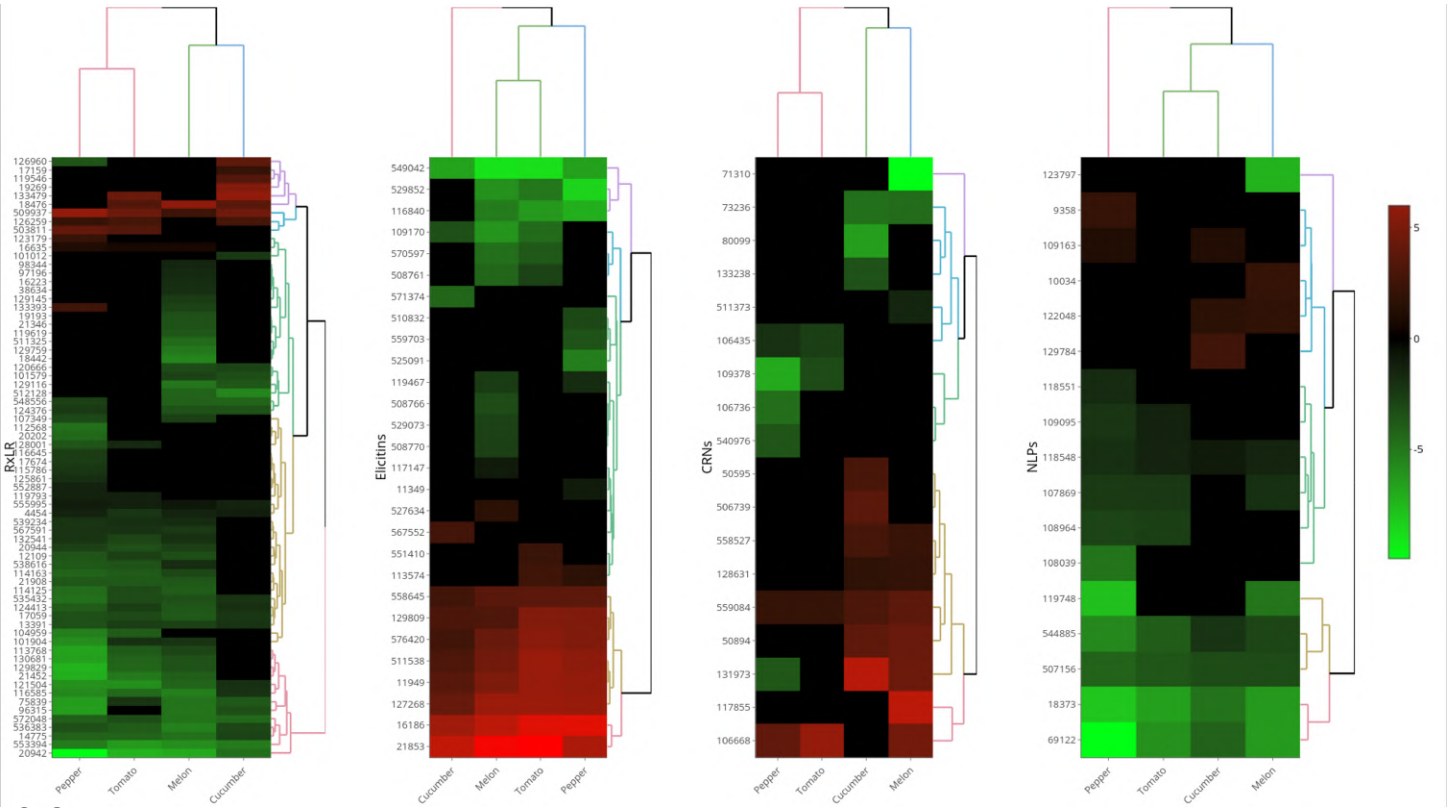

Figure 4: Heatmap of the Log2FC values of differentially expressed *Phytophthora* RxLR, elicitin, CRN, and NLP effectors.

321

322 **2.5 Host- and Tissue-Specific Phenotypes Associated with Effector Gene Silencing**

323 We investigated the role of four *P. capsici* genes by silencing via direct incubation with dsRNA.
324 The targeted genes included the differentially expressed necrosis- and ethylene-inducing peptide-
325 like protein (NLP Pc9358), induced exclusively in chili pepper; the RxLR effector Pc503811,
326 induced in chili pepper and tomato; the RxLR effector Pc18476, induced across all susceptible
327 hosts (cucumber, melon, and tomato) (Figure 4); and a non-differentially expressed conserved cell
328 cycle gene (Pc533030, encoding SDA1), known to be essential for sporangial morphology,
329 mycelial growth, and virulence (Zhu et al. 2016). Pathogen mycelia were incubated with the
330 corresponding dsRNAs for 2 h prior to infection assays on detached leaves and plantlet stems near
331 the crown to better mimic the conditions from previous experiments.

332 After 96 hpi, the control *P. capsici* grew on detached cucumber leaves. In contrast, all the
333 following dsRNA treatments decreased pathogen growth: Pc503811 (18.24%), Pc9358 (65.29%),
334 PcSDA1 (76.47%), and Pc18476 (78.82%) (Figure 5a, e). For detached tomato leaves measured
335 at 72 hpi, PcSDA1 dsRNA treatment unexpectedly resulted in a 10.58% increase in pathogen
336 growth, whereas the Pc503811 and Pc9358 treatments reduced growth by 76.51% and 84.6%,
337 respectively (Figure 5b, c, e).

338 In plantlet stem infection (96 hpi), cucumber did not differ between the dsRNA treatment groups
339 and the control group (Figure 5d, f). Similarly, in melon stems infected with dsRNA-treated
340 pathogen exhibited growth comparable to that of the control, although dsRNA treatments notably
341 prevented the appearance of necrosis. Conversely, in chili pepper and tomato stems, the PcSDA1
342 dsRNA-treated pathogen induced aggressive necrosis, surpassing the control severity and causing
343 complete tissue necrosis. In chili pepper, the Pc18476 and Pc503811 dsRNA treatments resulted
344 in reduced pathogen growth by 54% and 68%, respectively, but failed to prevent necrosis. Notably,
345 while the Pc9358 dsRNA treatment caused a more moderate 32% growth reduction, it completely
346 prevented necrosis in the chili pepper stems (Figure 5d, f). In tomato stems, dsRNA treatments
347 targeting Pc18476, Pc9358, and Pc503811 effectively prevented necrosis and resulted in pathogen
348 growth reductions of 18%, 34%, and 9%, respectively, relative to the control. Corroboration of
349 gene silencing induction by dsRNA treatment was performed via RT-qPCR (Figure 5g).

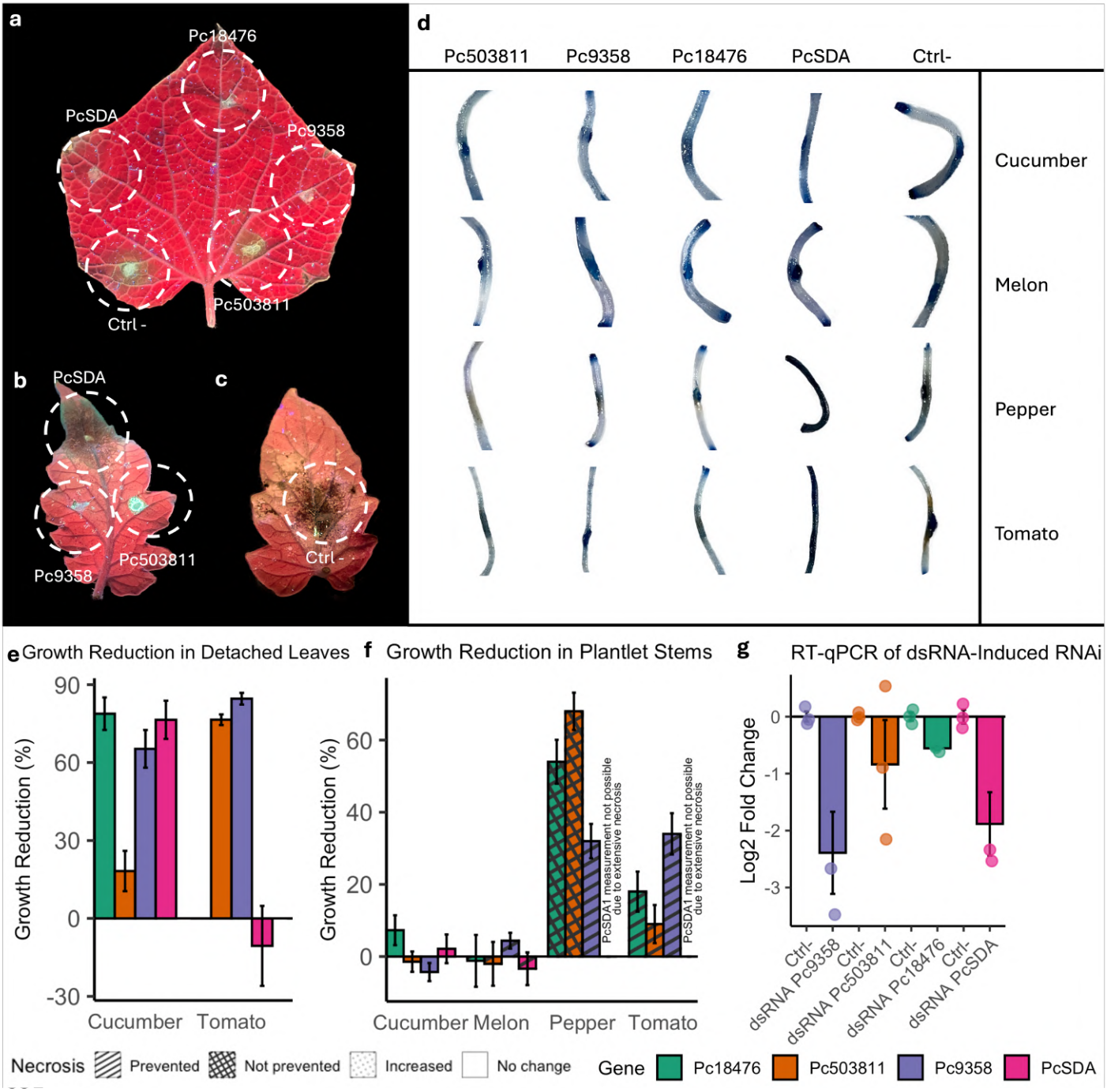

Figure 5: *P. capsici* gene-silenced phenotypes. **a** Cucumber detached leaf inoculated with *P. capsici* treated with dsRNAs targeting PcSDA, Pc18476, Pc9358 and Pc503811 or control plants treated with dsRNA buffer without dsRNA production after 96 hpi. **b** Tomato leaf inoculated with dsRNA-treated *P. capsici* after 72 hpi. **c** Tomato leaf inoculated with control *P. capsici* after 72 hpi. **d** Trypan blue-stained stems of cucumber, melon, tomato and chili pepper plantlets inoculated with

357 control or dsRNA-treated *P. capsici* after 96 hpi. **e** Growth reduction measurement of detached
358 leaves infected with dsRNA-treated *P. capsici*. **f** Growth reduction measurement of plantlet stems
359 infected with dsRNA-treated *P. capsici*.
360
361 **2.6 Co-expression analysis uncovers distinct transcriptional modules**
362 The co-expression analysis of *P. capsici* during infection of cucumber, melon, chili pepper, and
363 tomato revealed 10 distinct gene clusters with host-specific expression patterns and functional
364 enrichments. Cluster 1 (1,999 genes) is expressed at low levels in cucumber but is strongly induced
365 in melon, tomato, and chili pepper; it is enriched in processes such as ubiquitin-dependent protein
366 catabolism, vesicle-mediated transport and protein complex assembly. These functions, along with
367 pathways such as propanoate and fatty acid metabolism as well as secretion components, suggest
368 that in hosts other than cucumber, the pathogen deploys rapid protein turnover and secretion
369 mechanisms to modulate its virulence arsenal effectively (Figure 6).
370
371 Cluster 2 (1,096 genes) was mostly active in cucumber, with intermediate levels in melon and
372 tomato and low expression in chili pepper. The enrichment of translation and nitrogen metabolism
373 within this cluster implies a heightened emphasis on protein synthesis and energy acquisition
374 during the more tolerant, delayed infection observed in cucumber. Cluster 3 (832 genes) was
375 specifically upregulated in chili pepper and strongly enriched in central metabolic pathways,
376 including the tricarboxylic acid cycle, oxidative phosphorylation, and carbohydrate transport,
377 which may reflect an attempt by *P. capsici* to overcome the robust defense responses characteristic
378 of this partially resistant host.
379
380 A distinct transcriptional signature is observed during tomato infection, where cluster 4 of 984
381 genes is predominantly induced. The overrepresentation of genes involved in protein amino acid
382 phosphorylation, the ubiquitin cycle, and microtubule-based movement in this group suggests that
383 rapid cytoskeletal reorganization and signal transduction are critical for the early, aggressive
384 colonization that leads to swift necrosis in tomato. Moreover, cluster 5, with 902 genes highly
385 expressed in cucumber at intermediate levels in melon and chili pepper but low in tomato, was
386 enriched in pathways related to redox homeostasis, heme and pantothenate biosynthesis, and

387 glycolipid metabolism. This profile indicates that in cucumber, the lipid biosynthetic and redox-
388 balancing processes of the pathogen may be fine-tuned to support prolonged infection.
389
390 Cluster 6 with 741 genes upregulated in cucumber, melon, and chili pepper but repressed in tomato;
391 its enrichment in rRNA processing, ribosome biogenesis, transcription, and tRNA processing
392 underscores the importance of enhancing the pathogen's translational machinery in hosts where
393 colonization occurs over an extended period. Cluster 7 (603 genes), with moderate expression in
394 cucumber and high expression in melon and chili pepper, was associated with the modulation of
395 pathways such as porphyrin and pyrimidine metabolism, suggesting a role in fine-tuning gene
396 expression and nuclear-cytoplasmic transport in response to host defenses.
397
398 Notably, a large set of 967 genes in cluster 8 was highly expressed in cucumber, melon, and tomato
399 but was downregulated in chili pepper. This group was enriched for processes involved in cell
400 communication, protein phosphorylation, phospholipid transport, and carbohydrate metabolism,
401 along with nucleotide sugar and sphingoglycolipid metabolism. Such enrichment may reflect the
402 active remodeling of membranes and signaling networks to optimize effector secretion and host
403 interactions in more susceptible hosts. In addition, cluster 9, comprising 577 genes (upregulated
404 in cucumber, chili pepper, and tomato with low expression in melon), was enriched in pathways
405 including mismatch repair, defense response, glycolysis, cell wall modification, and pathogenesis
406 (Figure 6). Finally, a smaller, melon-specific cluster 10 of 381 genes, despite yielding no robust
407 enrichment.

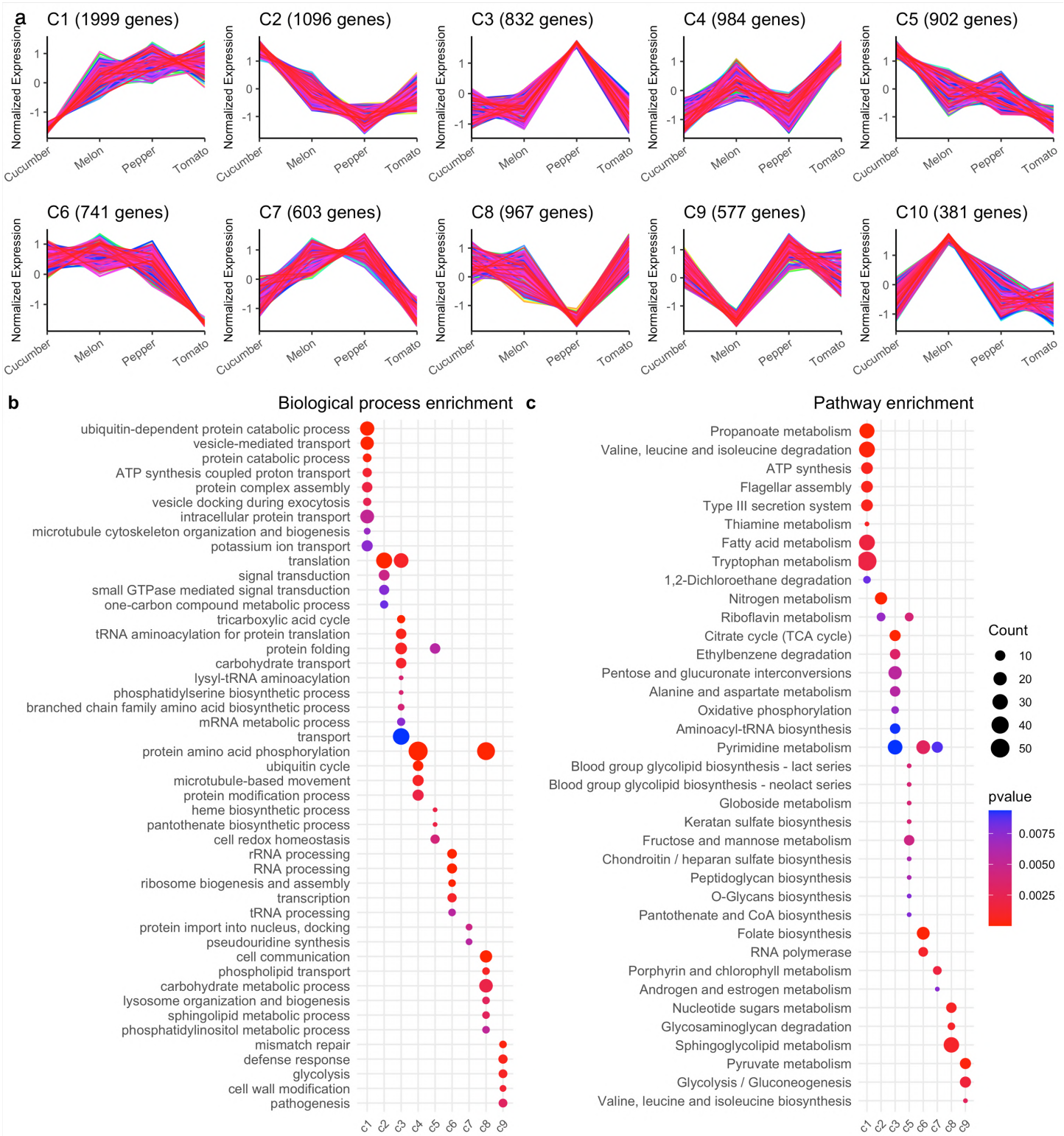
a
C1 (1999 genes)
C2 (1096 genes)
C3 (832 genes)
C4 (984 genes)
C5 (902 genes)
C6 (741 genes)
C7 (603 genes)
C8 (967 genes)
C9 (577 genes)
C10 (381 genes)
Normalized Expression
Cucumber
Melon
Pepper
Tomato
b
Biological process enrichment
ubiquitin-dependent protein catabolic process
vesicle-mediated transport
protein catabolic process
ATP synthesis coupled proton transport
protein complex assembly
vesicle docking during exocytosis
intracellular protein transport
microtubule cytoskeleton organization and biogenesis
potassium ion transport
translation
signal transduction
small GTPase mediated signal transduction
one-carbon compound metabolic process
tricarboxylic acid cycle
tRNA aminoacylation for protein translation
protein folding
carbohydrate transport
lysyl-tRNA aminoacylation
phosphatidylserine biosynthetic process
branched chain family amino acid biosynthetic process
mRNA metabolic process
transport
protein amino acid phosphorylation
ubiquitin cycle
microtubule-based movement
protein modification process
heme biosynthetic process
pantothenate biosynthetic process
cell redox homeostasis
rRNA processing
RNA processing
ribosome biogenesis and assembly
transcription
tRNA processing
protein import into nucleus, docking
pseudouridine synthesis
cell communication
phospholipid transport
carbohydrate metabolic process
lysosome organization and biogenesis
sphingolipid metabolic process
phosphatidylinositol metabolic process
mismatch repair
defense response
glycolysis
cell wall modification
pathogenesis
c
Pathway enrichment
Propanoate metabolism
Valine, leucine and isoleucine degradation
ATP synthesis
Flagellar assembly
Type III secretion system
Thiamine metabolism
Fatty acid metabolism
Tryptophan metabolism
1,2-Dichloroethane degradation
Nitrogen metabolism
Riboflavin metabolism
Citrate cycle (TCA cycle)
Ethylbenzene degradation
Pentose and glucuronate interconversions
Alanine and aspartate metabolism
Oxidative phosphorylation
Aminoacyl-tRNA biosynthesis
Pyrimidine metabolism
Blood group glycolipid biosynthesis - lact series
Blood group glycolipid biosynthesis - neolact series
Globoside metabolism
Keratan sulfate biosynthesis
Fructose and mannose metabolism
Chondroitin / heparan sulfate biosynthesis
Peptidoglycan biosynthesis
O-Glycans biosynthesis
Pantothenate and CoA biosynthesis
Folate biosynthesis
RNA polymerase
Porphyrin and chlorophyll metabolism
Androgen and estrogen metabolism
Nucleotide sugars metabolism
Glycosaminoglycan degradation
Sphingoglycolipid metabolism
Pyruvate metabolism
Glycolysis / Gluconeogenesis
Valine, leucine and isoleucine biosynthesis
c1 c2 c3 c4 c5 c6 c7 c8 c9
Count
10
20
30
40
50
pvalue
0.0075
0.0050
0.0025

Figure 6: Clustering of co-expressed genes based on their expression profiles across infected hosts. **a** Each panel represents a cluster (C1-C10) with the number of genes indicated in parentheses. **b** Biological process and **c** KEGG pathway enrichment of *P. capsici* cluster genes.

3 Discussion

3.1 Host-specific susceptibility and pathogen adaptation

Phytophthora capsici is a highly adaptable oomycete pathogen with a broad host range. This wide host range is facilitated by its ability to infect both root and aerial tissues, employ diverse infection strategies, and rapidly evolve virulence traits. However, the extent and nature of susceptibility vary markedly among host species and are influenced by both preformed defenses and inducible immune responses (Quesada-Ocampo et al. 2023). Our study demonstrated that host susceptibility to *P. capsici* is not a uniform phenomenon but is distinctly modulated by host species. In tomato plants, a Solanaceous host, necrosis is visible as early as 12 hours post-inoculation for some individuals, with a population median onset of 27 hpi, suggesting rapid cell death, which allows further pathogen colonization (Singh and Upadhyay 2014). In contrast, cucurbitaceous hosts (cucumber and melon) exhibit delayed necrosis (first symptoms at 36-48 hpi with medians ranging from 54 to 102 hpi), yet these hosts support extensive intracellular colonization. This combination of delayed cell death and significant intracellular proliferation may reflect a more tolerant interaction. As defined in plant pathology, tolerance refers to a plant's ability to endure the presence of a pathogen without suffering significant loss in yield or quality, even though the pathogen may still infect and reproduce within the plant (Pagán and García-Arenal 2018).

Our *Phytophthora* propagation findings in cucumber and melon align with previous studies that have documented a prolonged biotrophic phase in certain *Phytophthora* interactions. For example, in *P. infestans* infections of potato, delayed necrotic induction is associated with sustained colonization, which allows the pathogen to build a critical biomass before a switch to necrotrophy (Lee and Rose 2010; Schmelzer et al. 1995). In our system, the extensive vascular colonization observed in cucumber and melon via multiphoton microscopy suggests that these hosts may provide a relatively permissive environment that limits early defense activation. The result is a biotrophic scenario in which *P. capsici* can establish a systemic infection while minimizing the rapid release of damage-associated molecular patterns (DAMPs), which typically trigger strong

440 immune responses (Hernández-Chávez et al. 2017). Conversely, chili pepper (CM334), which was
441 previously characterized as partially resistant (López-Martínez et al. 2011), shows delayed
442 necrosis coupled with an absence of intracellular colonization. We indeed observed that *P. capsici*
443 was unable to penetrate chili pepper plants. These findings indicate that in resistant hosts,
444 preformed or induced defenses, such as reinforced cell walls and rapid antimicrobial signaling,
445 effectively restrict pathogen entry and subsequent proliferation.
446 Other studies have documented similar patterns. For example, (Maillot et al. 2022) compared the
447 transcriptomes of *P. capsici* strains infecting partially resistant CM334 chili peppers with those
448 infecting susceptible cultivars and reported that, in resistant tissues, the proliferation of the
449 pathogen was blocked early by rapid defense signaling. In contrast, in susceptible tissues, the
450 pathogen has the capacity to change the transcriptomic programming of the host response to delay
451 necrosis and establish more robust colonization. Our findings extend these observations to
452 cucurbits, suggesting that the apparent tolerance of cucumber and melon could allow pathogen
453 proliferation by a more extended period for nutrient use and colonization.

454 **3.2 Unique aspects of crown infection and broader implications**

455 A novel focus of our study was infection initiation at the stem base and root crown rather than in
456 foliar tissues. Most studies on *Phytophthora* have focused on leaf infections (Chen et al. 2018; Li
457 et al. 2020; Zhu et al. 2016). However, pathogens such as *P. capsici* are transmitted by the soil and
458 naturally target the crown region where roots and stem bases interface with the soil environment.
459 By examining these infection areas, we have uncovered critical insights into the early stages of
460 pathogen establishment. The crown region represents a crucial area with physical barriers and
461 localized immune responses that determine the success of infection (Bostock et al. 2014; Piccini
462 et al. 2019). In fact, the results here revealed that *P. capsici* can establish extensive intracellular
463 colonization in the crown of cucurbitaceous hosts without triggering rapid necrosis, suggesting
464 that these tissues may offer a relatively protected niche that permits sustained pathogen growth
465 and eventual systemic colonization. Understanding the dynamics of crown infection is particularly
466 important for developing targeted disease management strategies, potentially influencing
467 approaches to fungicide application and cultural practices.
468

Although zoospores are the primary dispersal and infection propagules of *P. capsici* in the field, we initiated infections with standardized mycelial amounts. This choice provided (i) a synchronized and reproducible infection starting across hosts with distinct surface chemistries, (ii) sufficient, clean pathogen RNA from the crown interface for comparative transcriptomics, and (iii) reduced variability due to zoospore encystment and germination kinetics. Under our conditions, mycelial inoculation consistently established crown colonization across species (Fig. 1a-d), enabling uniform sampling at 24 hpi. We therefore interpret our RNA-seq data as capturing host-conditioned crown-associated hyphae; we do not claim that they substitute for all aspects of zoospore-initiated infection in the field. Future work will explicitly compare zoospore- versus mycelium-initiated infections to dissect any inoculum-type effects on early transcriptional programs. These profiles primarily reflect hyphae exposed to host-derived cues at the infection interface, not isolated intracellular hyphae. This design allows for clean pathogen RNA recovery and host-matched comparisons, but it introduces an anatomical bias. Notably, our microscopy results revealed that at 24 hpi, cucurbits and tomatoes already exhibited abundant intercellular growth in stems 1 cm above the inoculation site (Fig. 1f–i; Fig. S1), whereas chili peppers did not, even upon later inspection (Fig. S2). Accordingly, we view our RNA-seq data as crown-interface, host-conditioned states that likely correlate with but do not fully encompass the transcriptional programs of invasive hyphae within each host. This caveat is especially relevant for pepper, where limited tissue ingress at 24–48 hpi suggests that external hyphae may dominate the sampled signal. Future experiments using tissue-enriched sampling will refine the in-planta compartment-specific programs.

3.3 Metabolic reprogramming and nutrient acquisition

The ability of *P. capsici* to reconfigure its metabolic networks in response to host-specific conditions emerged as another central theme of our work. In tomato, the upregulation of glycolytic and fatty acid metabolism pathways suggests rapid mobilization of energy and biosynthetic precursors to fuel aggressive colonization, a scenario commonly observed in necrotrophic interactions (Kwaik and Bumann 2015; Petrasch et al. 2019; Williams and Lorenz 2020). In cucurbits, however, our transcriptomic data revealed a pronounced enrichment of pathways related to carbohydrate metabolism, galactose utilization, and glycerolipid metabolism. These alterations may allow *P. capsici* to exploit the nutrient-rich vascular environment of cucumber and melon,

500 thereby supporting extensive intracellular colonization without triggering immediate cell death.
501 Such a strategy resembles the concept of "stealth colonization", wherein the pathogen minimizes
502 damage to host tissues to secure a longer-term nutritional niche (Petrasch et al. 2019; Williams and
503 Lorenz 2020).
504
505 In chili pepper (CM334, a genotype known to be partially resistant), the induction of metabolic
506 pathways associated with cell wall modification and nitrogen compound metabolism might reflect
507 adaptive responses to overcome the host's defensive mechanisms. It is likely that *P. capsici*
508 attempts to modify its own membranes and metabolic outputs to adapt better to a nutrient-scarce,
509 hostile environment imposed by robust host immunity. Such reprogramming may help to adapt to
510 a hostile microenvironment (Luo et al. 2021). This metabolic flexibility is emerging as a key
511 determinant of pathogen virulence and host adaptation, as has also been observed in other
512 oomycetes (Ah-Fong et al. 2017). The divergent metabolic signatures among hosts underscore the
513 plasticity of *P. capsici* physiology and its capacity to fine-tune nutrient acquisition strategies based
514 on host-derived signals. This versatility in metabolic reprogramming has been documented in other
515 soil-borne pathogens and is increasingly recognized as a key determinant of virulence and host
516 adaptation (Petrasch et al. 2019).
517
518 **3.4 Effector Dynamics and Host-Specific Virulence**
519 Effector proteins are key molecular tools employed by several pathogens to manipulate host
520 immunity and promote colonization. Oomycete effectors are broadly categorized into cytoplasmic
521 effectors and apoplastic effectors, depending on their localization and function (Bozkurt et al.
522 2011). Our transcriptomic analysis revealed that *P. capsici* effector expression is tightly regulated
523 in a host-dependent manner. Among effector proteins, RxLR effectors are of particular interest
524 because of their ability to translocate into host cells and suppress immune responses by targeting
525 host signaling pathways (Wang et al. 2023; Whisson et al. 2007). Our data show that while many
526 RxLR effectors are repressed, a subset is induced selectively depending on the host species. For
527 example, homologs of PcAvh328 (Pc123179, Pc128001, and Pc552887), which have been shown
528 to interfere with host defense signaling, displayed differential expression patterns, with at least one
529 homolog being induced in chili pepper. Such induction in a typically resistant host may represent
530 a targeted effort by the pathogen to counteract strong basal defenses. Two previously

uncharacterized RxLR effectors (Pc503811 and Pc18476) were selected for functional analysis via dsRNA-mediated silencing. Pc503811, which is induced specifically during infection in chili pepper and tomato, and Pc18476, which is expressed in cucumber, melon, and tomato infections, play distinct host-dependent roles. Silencing of Pc503811 resulted in a modest (18%) reduction in pathogen growth on detached cucumber leaves, whereas a substantial 76% growth reduction was observed on detached tomato leaves. During stem infection of cucumber plantlets, silencing Pc503811 had no significant effect on pathogen growth. However, in melon stems, although pathogen growth remained comparable to that of the control, necrosis development was prevented. Notably, in chili pepper stems, pathogen growth was notably reduced, and in tomato stems, both pathogen growth reduction and necrosis prevention were observed. These results suggest that the function of Pc503811 may be particularly relevant in interactions with solanaceous hosts. The effector Pc18476, which is induced in all susceptible hosts, also has host- and tissue-dependent effects when silenced via dsRNA. In detached cucumber leaves, Pc18476 dsRNA treatment resulted in a substantial 78% reduction in pathogen growth; however, this treatment had no detectable effect on pathogen growth during infection of cucumber plantlet stems. In melon stems, pathogen growth was like in controls, yet necrosis development was prevented by dsRNA treatment. In chili pepper stems, pathogen growth was reduced by 54%, whereas in tomato stems, growth was modestly reduced by 18%, but importantly, necrosis was completely prevented.

PcAvh16 homologs (Pc14944, Pc14948, and Pc533084), which are implicated in the suppression of programmed cell death (Wang et al. 2011), are differentially regulated, suggesting that *P. capsici* tailors its effector deployment to prolong its biotrophic phase, particularly in hosts with rapid necrotic responses like tomato. In contrast, the consistent downregulation of effectors such as PcAvh166 across hosts may indicate roles confined to early infection events or environmental conditions not captured at our 24 hpi sampling. Moreover, our observations of elicitins (INF1 and INF2B) and Nep1-like proteins (NLPs) underscore the complexity of effector regulation. Canonical elicitins are well known from *P. infestans* to induce hypersensitive responses (Derevnina et al. 2016; Du et al. 2017; Huitema et al. 2005); their repression in cucurbits could be interpreted as deliberate suppression to avoid triggering host defenses prematurely. In contrast, the unique induction of PcNLP14 in chili pepper may represent a specialized mechanism to manipulate host cell death pathways and modulate immune responses (Chen et al. 2018).

562

563 The NLP effector Pc9358, which is specifically induced during infections of chili pepper, exhibited
564 host- and tissue-dependent phenotypes when silenced by dsRNA. On detached cucumber leaves,
565 Pc9358 silencing caused a 65% reduction in pathogen growth, although no effect was observed on
566 cucumber plantlet stems. In melon stems, pathogen growth was unaffected by dsRNA treatment,
567 but the induction of necrosis was completely prevented. In chili pepper and tomato stems, Pc9358
568 silencing reduced pathogen growth by 32% and 34%, respectively, and prevented necrosis
569 development in both hosts. Interestingly, this was the only effective silencing treatment that
570 successfully prevented necrosis in chili pepper stems.

571

572 We also selected Pc533030, encoding the conserved cell cycle regulator SDA1, as a control for
573 evaluating the efficacy of dsRNA treatments on pathogen growth. This gene was non-differentially
574 expressed in our transcriptomic datasets but was previously shown to be essential for sporangial
575 morphology, mycelial growth, and virulence during susceptible chili pepper leaf infections (Zhu
576 et al. 2016). Treatment of *P. capsici* with PcSDA1 dsRNA resulted in a 76% reduction in pathogen
577 growth on detached cucumber leaves; however, pathogen growth unexpectedly increased by 10%
578 in tomato leaves. In plantlet stems, PcSDA1 dsRNA treatment caused severe and aggressive
579 necrosis in chili peppers and tomatoes, surpassing control infections and leading to complete tissue
580 necrosis. No changes were observed in the cucumber stems, whereas necrosis was prevented in
581 the melon stems.

582

583 The growth reduction observed in cucumber leaves is consistent with previous findings that SDA1
584 is critical for hyphal development and virulence. However, the increased growth in tomato leaves
585 and exacerbated necrosis in tomato and chili stems are unexpected and may reflect a compensatory
586 or stress-induced hypervirulence response when the cell cycle is disrupted (Goncheva et al. 2019).
587 This raises the possibility that interference with essential cellular functions in *P. capsici* might
588 dysregulate effector release or stress signaling, enhancing host tissue damage in some contexts
589 (Goncheva et al. 2019). Conversely, the absence of necrosis in melon stems might indicate a
590 differential host response to weakened or developmentally impaired pathogen tissue. Altogether,
591 these findings illustrate the complexity of targeting conserved genes and highlight that silencing

592 even core regulators like SDA1 can lead to variable outcomes depending on the infection
593 environment, host genotype, or tissue type.
594
595 Recent reviews have described that the spatial and temporal regulation of effectors is crucial for
596 pathogen success (Wang et al. 2023). Our study extends these findings by demonstrating that the
597 expression profiles of effectors are not only host-specific but may also be influenced by the
598 infection niche, in our case, the crown region comprising the stem base and roots. This localized
599 deployment of effectors may reflect an adaptation to the unique defense barriers and nutrient
600 landscapes encountered at the soil-plant interface, where rapid colonization of vascular tissues can
601 be pivotal for systemic infection.
602
603 **4 Conclusions**
604 We found that *Phytophthora capsici* has developed an adaptive strategy to colonize diverse plant
605 species. In tomato, rapid necrosis limits pathogen spread, yet aggressive metabolic reprogramming
606 supports early infection. On the other hand, the slow necrosis induction in cucumber and melon
607 coupled with extensive intercellular colonization points to a tolerance interaction that may
608 facilitate prolonged pathogen proliferation. In the partially resistant chili pepper CM334, robust
609 defense mechanisms inhibit intercellular colonization despite transcriptional changes in the
610 pathogen. Our comprehensive pathogen-centered transcriptomic analysis revealed that differential
611 effector deployment, metabolic reprogramming, and nutrient acquisition strategies are key
612 components of *P. capsici* adaptive virulence. This study highlights the value of examining the
613 transcriptional dynamics of pathogens, an approach often overlooked in favor of host-focused
614 analyses. By focusing on crown infections, this work expands our understanding of soil-borne
615 infection dynamics, a perspective that has been underrepresented in studies that predominantly
616 target foliar diseases.
617

618 **5 Materials and methods**

619 **5.1 Strains, media and culture conditions**

620 The *Phytophthora capsici* strain used in this study was D3 mating type A1 (Pons-Hernández et al.
621 2020; Sevillano-Serrano et al. 2024). *P. capsici* D3 was routinely grown on V8 agar in the dark at
622 24°C.

623

624 **5.2 Infection assay**

625 To infect seedlings with *P. capsici* D3, 0.01 g of mycelium from 5-day-old cultures was harvested
626 with tweezers and deposited in the crown of 5-8 weeks-old seedlings. Plants used as hosts in the
627 present study were *Capsicum annuum* (Criollo de Morelos 334), *Cucumis melo*, *Cucumis sativus*,
628 and *Solanum lycopersicum*. As a non-plant infection control, the same mycelium source was
629 cultivated on V8 agar plates. At 24 hours post-inoculation, the accessible mycelium on the infected
630 plant surface was recovered with tweezers for subsequent RNA extraction. To quantify necrosis at
631 the crown, the plants were inspected at fixed intervals (every 6 h from 6-144 hpi). At each
632 timepoint, a 50 mm segment encompassing the stem base and upper root segment centered on the
633 inoculation site was excised and processed as follows to visualize dead cells: tissues were cleared
634 overnight in acetic acid:ethanol (1:3, v/v) and then transferred to acetic acid:ethanol:glycerol
635 (1:5:1, v/v/v) for 3 h. Cleared samples were stained for 3 h in 0.01% (w/v) trypan blue and stored
636 in 60% glycerol until examination. Stained tissues were imaged at constant magnification via a
637 bright-field microscope. Necrosis onset (event) was defined a priori as the earliest timepoint at
638 which a contiguous trypan blue-positive band of ≥2.0 mm in longitudinal extent was present at the
639 inoculation zone. Quantification was performed in ImageJ by RGB channel separation and
640 intensity-thresholding of the blue channel within a fixed ROI (50 mm length × full stem width).
641 For each host and time, 3 plants were scored across 3 independent experiments.

642

643 **5.3 Multiphoton microscopy**

644 Stems and roots were dissected from 1 cm from the crown inoculation site. The samples were fixed
645 in 4% paraformaldehyde and incubated for 2 h. Subsequently, the samples were washed with 0.16
646 M phosphate buffer at pH 7.2, embedded in Sakura Tissue Tek, and frozen at -20°C. The samples
647 were sectioned in a cryotome to a width of 100 µm. The tissue sections were stained with
648 propidium iodine (IP) at a final concentration of 0.0003%. To stain the cell wall, the samples were

649 treated with 0.01% Solophenyl. The stained samples were visualized via an LSM 880-NLO Axio
650 Imager Z2 microscope (Zeiss, Oberkochen, Germany) coupled to a Ti:Sapphire infrared laser
651 (Chameleon Vision II, COHERENT, Santa Clara, CA, USA). The excitation laser was set at 543
652 nm for propidium iodine and 458 nm for the solophenyl. The emission ranged from 548 to 684 for
653 IP and 502 to 558 nm for the solophenyl. All the micrographs were captured in CZI format at 1131
654 × 1131 pixels and RGB color. The spectral graphs were analyzed via SigmaPlot 12 (Systat
655 Software, Inc.).
656
657 **5.4 RNA extraction and Illumina sequencing**
658 Total RNA was extracted via the Quick-RNA Plant Miniprep Kit (Zymo Research, CA, USA)
659 according to the manufacturer's protocol, omitting the Zymo-Spin III-HRC column in the final
660 step. Mycelia of 10 infected plants were pooled per extraction, and 0.1 g of mycelia was used for
661 each extraction; mycelia were harvested at 12:00 (±1 hr), immediately flash-frozen in liquid
662 nitrogen, and processed without thawing. The RNA quality was measured with a Bioanalyzer, and
663 samples with a RIN > 5 were used for sequencing. RNA-Seq libraries (15 libraries in total,
664 representing five conditions with three biological replicates per condition) were prepared by
665 selectively isolating mRNA via poly-T oligo-attached magnetic beads. Libraries were sequenced
666 at Novogene (Sacramento, CA, USA) via the Illumina NovaSeq 6000 platform (Hayward, CA,
667 USA), generating paired-end reads (2 × 150 bp) with an average yield of 50 million reads per
668 library. The raw sequencing data have been deposited in the NCBI database under BioProject
669 accession number PRJNA1207595.
670
671 **5.5 Mapping and statistical analysis**
672 Read trimming and adaptor removal were performed using BBDuk with the following parameters:
673 `forcetrimleft=20` and `trimq=20` (https://sourceforge.net/projects/bbmap/). Mapping and
674 quantification were conducted with Kallisto via the *P. capsici* LT1534 v11.0 transcriptome
675 (available at MycoCosm: mycocosm.jgi.doe.gov) (Bray et al. 2016; Grigoriev et al. 2014; Lamour
676 et al. 2012a), employing bias correction and 100 bootstrap replicates. Approximately 77% of the
677 reads were pseudoaligned to the transcriptome. Differential expression analysis was carried out
678 via DESeq2, as described previously (Love et al. 2014; Tanja 2023). *P. capsici* grown on V8 agar
679 served as the control condition. Transcripts with an adjusted p value (p value) ≤ 0.05 and a

680 log2FoldChange > 1 or < -1 were considered differentially expressed genes (DEGs). Co-
681 expression analysis was executed with Clust 1.18, using the parameters `-no optimization`
682 (Abu-Jamous and Kelly 2018).
683
684 **5.6 Functional enrichment**
685 To identify gene ontology (GO) terms and enriched KEGG pathways, the reference transcriptome
686 was reannotated via eggNOG mapper v2.1.12 (Huerta-Cepas et al. 2019) and merged with existing
687 MycoCosm annotations. Effector proteins, including RXLRs, CRNs, Elicitins, and Nep1-like
688 proteins (NLPs), were retrieved from the literature and supplemented by identifying additional
689 candidates using EffectorP v3.0. Additional secreted proteins were predicted via SignalP v6
690 (Sperschneider and Dodds 2022; Teufel et al. 2022). Functional enrichment analysis was
691 performed with clusterProfiler v4.12.6, employing an over-representation analysis (ORA)
692 approach and applying a *p* value cutoff of ≤0.05 (Wu et al. 2021). Effectors were annotated against
693 various databases with BLAST using an e-value < $1x10^{-30}$.
694
695 **5.7 Functional validation by RNAi**
696 Functional validation by gene silencing of three effector genes was conducted by designing RNAi
697 sequences and their respective primers using SIREN v0.1.5
698 (https://github.com/pablovargasmejia/SIREN), and the T7 promoter was added to each primer
699 (Table S1). To avoid off-target effects on the pathogen and host plants, an off-target database was
700 constructed with the cDNA sequences of *P. capsici* and the four host plants with the --targets option
701 in SIREN v0.1.5. Designed RNAi sequences were transcribed *in vitro* from *P. capsici* cDNA fused
702 with the T7 promoter using HighYield T7 RNAi Kit at 37°C for 4 h (Jena Bioscience, Germany).
703 RNAi experiments were performed as follows: 1 µg of synthetic dsRNA was incubated with 0.1 g
704 of *P. capsici* mycelium for 2 h on ice to facilitate cellular uptake. Then, 0.01 g of treated mycelium
705 was used as inoculum for virulence assays on adult plant leaves or plantlet stems. As a negative
706 control for silencing, *P. capsici* mycelium was incubated as described with T7 reaction components
707 that excluded RNA production. To screen the disease phenotype of the silenced genes, inoculated
708 leaves and stems were first cleared in an acetic acid:ethanol (1:3, v/v) solution overnight and then
709 in an acetic acid:ethanol:glycerol (1:5:1, v/v/v) solution for 3 h. The samples were subsequently

710 incubated for 3 h in a staining solution of 0.01% (w/v) trypan blue and then stored in 60% glycerol
711 until examination.
712 The reduction in target gene transcript levels following dsRNA treatment was quantified via
713 RT-qPCR using the comparative **ΔΔ**C_t method. The elongation factor 1 gene served as an
714 endogenous gene. The oligonucleotide sequences are provided in Table S2. For each assay, three
715 biological replicates were sampled at 6 hours post-inoculation (hpi) from either dsRNA-treated or
716 control *P. capsici* mycelial inoculum. Total RNA was extracted as described previously, and 1 µg
717 of RNA was reverse transcribed using the Jena SCRIPT cDNA Synthesis Kit (Jena Bioscience,
718 Germany). Quantitative PCR was performed on an Applied Biosystems StepOne Real-Time PCR
719 System (Thermo Fisher Scientific, USA), employing the qPCR GreenMaster highROX from Jena.
720 Reaction conditions and cycling parameters followed the manufacturer's guidelines.
721
722 **Declaration of competing interest**
723 The authors declare no conflict of interest.
724
725 **Availability of data and materials**
726 The raw reads generated during the current study are publicly available at NCBI under the
727 PRJNA1207595 accession number. Materials are available from the corresponding author upon
728 reasonable request.
729 https://dataview.ncbi.nlm.nih.gov/object/PRJNA1207595?reviewer=34591133boj3j0q7vu5nrpi1t
730 p
731
732 **Acknowledgments**
733 This work forms part of the requirements for P.V.M. to obtain a Doctoral degree from the Posgrado
734 en Ciencias Biológicas program at Universidad Nacional Autónoma de México (UNAM). P.V.M.
735 receives a doctoral scholarship from Secretaria de Ciencia, Humanidades, Tecnología e Innovación
736 (SECIHTI). F.U.R.R. receives a posdoctoral fellowship from "Estancias Posdoctorales por México
737 2022" supported by SECIHTI. Funding was provided by PAPIIT-DGAPA-UNAM (project
738 IN218024) and SECIHTI (project A1-S-34759) to JV-A.
739
740 **References**

741 Abu-Jamous B, Kelly S. Clust: automatic extraction of optimal co-expressed gene clusters from
742 gene expression data. Genome Biology. 2018 Oct 25;19(1):172.

743 Ah-Fong AMV, Boyd AM, Matson MEH, Judelson HS. A Cas12a-based gene editing system for
744 Phytophthora infestans reveals monoallelic expression of an elicitor. Molecular Plant Pathology.
745 2021;22(6):737–52.

746 Ah-Fong AMV, Kim KS, Judelson HS. RNA-seq of life stages of the oomycete Phytophthora
747 infestans reveals dynamic changes in metabolic, signal transduction, and pathogenesis genes
748 and a major role for calcium signaling in development. BMC Genomics. 2017 Feb 23;18(1):198.

749 Bostock RM, Pye MF, Roubtsova TV. Predisposition in Plant Disease: Exploiting the Nexus in
750 Abiotic and Biotic Stress Perception and Response. Annual Review of Phytopathology. Annual
751 Reviews; 2014 Aug 4;52(Volume 52, 2014):517–49.

752 Bozkurt TO, Schornack S, Win J, Shindo T, Ilyas M, Oliva R, et al. Phytophthora infestans effector
753 AVRblb2 prevents secretion of a plant immune protease at the haustorial interface. Proceedings
754 of the National Academy of Sciences. Proceedings of the National Academy of Sciences; 2011
755 Dec 20;108(51):20832–7.

756 Bray NL, Pimentel H, Melsted P, Pachter L. Near-optimal probabilistic RNA-seq quantification.
757 Nature Biotechnology. 2016 May;34(5):525–7.

758 Chen X, Li Y, Xing Y, Xu J, Tong Y. Cloning, transcriptional profiles and roles of *Phytophthora*
759 *capsici* CRN-encoding genes in the interaction with host plants. Acta Phytopathologica Sinica.
760 2015 Aug 10;45(4):384–94.

761 Chen X-R, Huang S-X, Zhang Y, Sheng G-L, Li Y-P, Zhu F. Identification and functional analysis of
762 the NLP-encoding genes from the phytopathogenic oomycete Phytophthora capsici. Mol Genet
763 Genomics. 2018 Aug;293(4):931–43.

764 Chen X-R, Xing Y-P, Li Y-P, Tong Y-H, Xu J-Y. RNA-Seq Reveals Infection-Related Gene Expression
765 Changes in Phytophthora capsici. PLOS ONE. Public Library of Science; 2013 Sept 3;8(9):e74588.

766 Chepsergon J, Motaung TE, Moleleki LN. “Core” RxLR effectors in phytopathogenic oomycetes: A
767 promising way to breeding for durable resistance in plants? Virulence. 12(1):1921–35.

768 Derevnina L, Dagdas YF, De la Concepcion JC, Bialas A, Kellner R, Petre B, et al. Nine things to
769 know about elicitins. New Phytologist. 2016;212(4):888–95.

770 Du J, Guo X, Chen L, Xie C, Liu J. Proteomic analysis of differentially expressed proteins of
771 Nicotiana benthamiana triggered by INF1 elicitin from Phytophthora infestans. J Gen Plant
772 Pathol. 2017 Mar 1;83(2):66–77.

773 Fedkenheuer KE. Molecular Analysis of Oomycete Pathogens to Identify and Translate Novel
774 Resistance Mechanisms to Crops. Virginia Tech; 2016 July 14 [cited 2025 Feb 23]; Available from:
775 http://hdl.handle.net/10919/81548

776 Feng B-Z, Zhu X-P, Fu L, Lv R-F, Storey D, Tooley P, et al. Characterization of necrosis-inducing NLP
777 proteins in Phytophthora capsici. BMC Plant Biol. 2014 May 8;14(1):126.

778 Goncheva MI, Flannagan RS, Sterling BE, Laakso HA, Friedrich NC, Kaiser JC, et al. Stress-induced
779 inactivation of the Staphylococcus aureus purine biosynthesis repressor leads to hypervirulence.
780 Nat Commun. Nature Publishing Group; 2019 Feb 15;10(1):775.

781 Grigoriev IV, Nikitin R, Haridas S, Kuo A, Ohm R, Otillar R, et al. MycoCosm portal: gearing up for
782 1000 fungal genomes. Nucleic Acids Research. 2014 Jan 1;42(D1):D699–704.

783 Hausbeck MK, Lamour KH. Phytophthora capsici on Vegetable Crops: Research Progress and
784 Management Challenges. Plant Disease. Scientific Societies; 2004 Dec;88(12):1292–303.

785 Hernández-Chávez MJ, Pérez-García LA, Niño-Vega GA, Mora-Montes HM. Fungal Strategies to
786 Evade the Host Immune Recognition. Journal of Fungi. Multidisciplinary Digital Publishing
787 Institute; 2017 Dec;3(4):51.

788 Huerta-Cepas J, Szklarczyk D, Heller D, Hernández-Plaza A, Forslund SK, Cook H, et al. eggNOG
789 5.0: a hierarchical, functionally and phylogenetically annotated orthology resource based on
790 5090 organisms and 2502 viruses. Nucleic Acids Res. 2019 Jan 8;47(D1):D309–14.

791 Huitema E, Vleeshouwers VGAA, Cakir C, Kamoun S, Govers F. Differences in Intensity and
792 Specificity of Hypersensitive Response Induction in Nicotiana spp. by INF1, INF2A, and INF2B of
793 Phytophthora infestans. MPMI. Scientific Societies; 2005 Mar;18(3):183–93.

794 Judelson HS. Metabolic Diversity and Novelties in the Oomycetes. Annual Review of
795 Microbiology. Annual Reviews; 2017 Sept 8;71(Volume 71, 2017):21–39.

796 Jupe J, Stam R, Howden AJ, Morris JA, Zhang R, Hedley PE, et al. Phytophthora capsici-tomato
797 interaction features dramatic shifts in gene expression associated with a hemi-biotrophic
798 lifestyle. Genome Biology. 2013 June 25;14(6):R63.

799 Knight NL, Sutherland MW. Histopathological Assessment of Fusarium pseudograminearum
800 Colonization of Cereal Culms During Crown Rot Infections. Plant Disease. Scientific Societies;
801 2016 Feb;100(2):252–9.

802 Kwaik YA, Bumann D. Host Delivery of Favorite Meals for Intracellular Pathogens. PLOS
803 Pathogens. Public Library of Science; 2015 June 25;11(6):e1004866.

804 Lamour KH, Mudge J, Gobena D, Hurtado-Gonzales OP, Schmutz J, Kuo A, et al. Genome
805 sequencing and mapping reveal loss of heterozygosity as a mechanism for rapid adaptation in

806 the vegetable pathogen Phytophthora capsici. Mol Plant Microbe Interact. 2012a
807 Oct;25(10):1350–60.

808 Lamour KH, Stam R, Jupe J, Huitema E. The oomycete broad-host-range pathogen Phytophthora
809 capsici. Mol Plant Pathol. 2012b May;13(4):329–37.

810 Lee S-J, Rose JKC. Mediation of the transition from biotrophy to necrotrophy in hemibiotrophic
811 plant pathogens by secreted effector proteins. Plant Signaling & Behavior. Taylor & Francis; 2010
812 June 1;5(6):769–72.

813 Lenarčič T, Albert I, Böhm H, Hodnik V, Pirc K, Zavec AB, et al. Eudicot plant-specific sphingolipids
814 determine host selectivity of microbial NLP cytolysins. Science. American Association for the
815 Advancement of Science; 2017 Dec 15;358(6369):1431–4.

816 Li Q, Wang J, Bai T, Zhang M, Jia Y, Shen D, et al. A Phytophthora capsici effector suppresses
817 plant immunity via interaction with EDS1. Molecular Plant Pathology. 2020;21(4):502–11.

818 López-Martínez N, Colinas-León MaT, Peña-Valdivia CB, Salinas-Moreno Y, Fuentes-Montiel P,
819 Biesaga M, et al. Alterations in peroxidase activity and phenylpropanoid metabolism induced by
820 Nacobbus aberrans Thorne and Allen, 1944 in chilli (Capsicum annuum L.) CM334 resistant to
821 Phytophthora capsici Leo. Plant Soil. 2011 Jan 1;338(1):399–409.

822 Love MI, Huber W, Anders S. Moderated estimation of fold change and dispersion for RNA-seq
823 data with DESeq2. Genome Biology. 2014 Dec 5;15(12):550.

824 Luo M, Sun X, Qi Y, Zhou J, Wu X, Tian Z. Phytophthora infestans RXLR effector Pi04089 perturbs
825 diverse defense-related genes to suppress host immunity. BMC Plant Biol. 2021 Dec 9;21(1):582.

826 Maillot G, Szadkowski E, Massire A, Brunaud V, Rigaill G, Caromel B, et al. Strive or thrive: Trends
827 in Phytophthora capsici gene expression in partially resistant pepper. Frontiers in Plant Science
828 [Internet]. 2022 [cited 2022 Nov 22];13. Available from:
829 https://www.readcube.com/articles/10.3389%2Ffpls.2022.980587

830 Pagán I, García-Arenal F. Tolerance to Plant Pathogens: Theory and Experimental Evidence.
831 International Journal of Molecular Sciences. Multidisciplinary Digital Publishing Institute; 2018
832 Mar;19(3):810.

833 Petrasch S, Silva CJ, Mesquida-Pesci SD, Gallegos K, van den Abeele C, Papin V, et al. Infection
834 Strategies Deployed by Botrytis cinerea, Fusarium acuminatum, and Rhizopus stolonifer as a
835 Function of Tomato Fruit Ripening Stage. Front. Plant Sci. [Internet]. Frontiers; 2019 Mar 1 [cited
836 2025 Feb 23];10. Available from: https://www.frontiersin.org/journals/plant-
837 science/articles/10.3389/fpls.2019.00223/full

838 Piccini C, Parrotta L, Faleri C, Romi M, Del Duca S, Cai G. Histomolecular responses in susceptible
839 and resistant phenotypes of *Capsicum annuum* L. infected with *Phytophthora capsici*. Scientia
840 Horticulturae. 2019 Jan 26;244:122–33.

841 Pons-Hernández JL, Guerrero-Aguilar BZ, González-Chavira MM, González-Pérez E, Villalobos-
842 Reyes S, Muñoz-Sánchez CI, et al. Phenotypic variability of Phytophthora capsici isolates in
843 Guanajuato. Revista mexicana de ciencias agrícolas. Instituto Nacional de Investigaciones
844 Forestales, Agrícolas y Pecuarias; 2020 Dec;11(8):1891–901.

845 Quesada-Ocampo LM, Parada-Rojas CH, Hansen Z, Vogel G, Smart C, Hausbeck MK, et al.
846 Phytophthora capsici: Recent Progress on Fundamental Biology and Disease Management 100
847 Years After Its Description. Annu Rev Phytopathol. 2023 Sept 5;61:185–208.

848 Schmelzer E, Naton B, Freytag S, Rouhara I, Küster B, Hahlbrock K. Infection-induced rapid cell
849 death in plants: a means of efficient pathogen defense. Can. J. Bot. NRC Research Press; 1995
850 Dec 31;73(S1):426–34.

851 Sevillano-Serrano J, Larsen J, Rojas-Rojas FU, Vega-Arreguín JC. Increasing virulence and
852 decreasing fungicide sensitivity in Phytophthora capsici after continuous metalaxyl-
853 chlorothalonil exposure. J Plant Pathol. 2024 Nov 1;106(4):1583–90.

854 Singh VK, Upadhyay RS. Fusaric acid induced cell death and changes in oxidative metabolism of
855 Solanum lycopersicum L. Botanical Studies. 2014 Aug 27;55(1):66.

856 Sperschneider J, Dodds PN. EffectorP 3.0: Prediction of Apoplastic and Cytoplasmic Effectors in
857 Fungi and Oomycetes. MPMI. Scientific Societies; 2022 Feb;35(2):146–56.

858 Stam R, Motion GB, Martinez-Heredia V, Boevink PC, Huitema E. A Conserved Oomycete CRN
859 Effector Targets Tomato TCP14-2 to Enhance Virulence. Mol Plant Microbe Interact. 2021
860 Mar;34(3):309–18.

861 Stephens AE, Gardiner DM, White RG, Munn AL, Manners JM. Phases of Infection and Gene
862 Expression of Fusarium graminearum During Crown Rot Disease of Wheat. MPMI. Scientific
863 Societies; 2008 Dec;21(12):1571–81.

864 Tanja S. Differential Gene Expression Analysis with Kallisto & DESeq2 [Internet]. 2023 [cited
865 2024 Oct 3]. Available from: https://rstudio-pubs-
866 static.s3.amazonaws.com/1028886_a1d8cbab80fe4742bfec36e0503b3a4e.html

867 Teufel F, Almagro Armenteros JJ, Johansen AR, Gíslason MH, Pihl SI, Tsirigos KD, et al. SignalP 6.0
868 predicts all five types of signal peptides using protein language models. Nat Biotechnol. Nature
869 Publishing Group; 2022 July;40(7):1023–5.

870 Wang Q, Han C, Ferreira AO, Yu X, Ye W, Tripathy S, et al. Transcriptional Programming and
871 Functional Interactions within the Phytophthora sojae RXLR Effector Repertoire. The Plant Cell.
872 2011 June 1;23(6):2064–86.

873 Wang S, McLellan H, Boevink PC, Birch PRJ. RxLR Effectors: Master Modulators, Modifiers and
874 Manipulators. Mol Plant Microbe Interact. 2023 Dec;36(12):754–63.

875 Whisson SC, Boevink PC, Moleleki L, Avrova AO, Morales JG, Gilroy EM, et al. A translocation
876 signal for delivery of oomycete effector proteins into host plant cells. Nature. 2007 Nov
877 1;450(7166):115–8.

878 Williams RB, Lorenz MC. Multiple Alternative Carbon Pathways Combine To Promote Candida
879 albicans Stress Resistance, Immune Interactions, and Virulence. mBio. American Society for
880 Microbiology; 2020 Jan 14;11(1):10.1128/mbio.03070-19.

881 Wu T, Hu E, Xu S, Chen M, Guo P, Dai Z, et al. clusterProfiler 4.0: A universal enrichment tool for
882 interpreting omics data. Innovation [Internet]. Elsevier; 2021 Aug 28 [cited 2022 Nov 10];2(3).
883 Available from: https://www.cell.com/the-innovation/abstract/S2666-6758(21)00066-7

884 Zhu C, Yang X, Lv R, Li Z, Ding X, Tyler BM, et al. hytophthora capsici homologue of the cell cycle
885 regulator 1 is required for sporangial morphology, mycelial growth and plant infection.
886 Molecular Plant Pathology. 2016;17(3):369–87.

887 Zuluaga AP, Vega-Arreguín JC, Fei Z, Ponnala L, Lee SJ, Matas AJ, et al. Transcriptional dynamics
888 of Phytophthora infestans during sequential stages of hemibiotrophic infection of tomato. Mol
889 Plant Pathol. 2016 Jan;17(1):29–41.

890